A Density Functional Theory Study of the Radiation Products of Glycine

Fuqiang Ban, James W. Gauld, and Russell J. Boyd*

Department of Chemistry, Dalhousie University, Halifax, NS, Canada B3H 4J3

Received: October 29, 1999; In Final Form: January 13, 2000

Density functional theory was employed to investigate the radicals that have been proposed to be formed upon irradiation of glycine crystals. The present theoretical study suggests that the radicals are R1: $^{+}NH_3C^{\bullet}HCOO^{-}$; R2: $^{\bullet}CH_2COOH$; R3: $NH_2C^{\bullet}HCOOH$; and R4: $NH_2CH_2COC^{\bullet}HCOOH$. A C_s structure for R1, obtained using the Onsager model, gives hyperfine coupling constants in agreement with experiment. Hyperfine coupling constants computed for R2 are in agreement with the unassigned experimental data of Teslenko, V. V. et al. (*Mol. Phys*. **1975**, *30*, 425). The computed hyperfine coupling constants for R4 are in good agreement with the experimental data assigned to the zwitterionic form $^{+}NH_3CH_2COC^{\bullet}HCOO^{-}$. It is shown that the structure of R3 is influenced significantly by the glycine crystal environment. Protonation of R3 gives rise to hyperfine couplings similar to the experimental values assigned to one conformer of R3.

Introduction

Recently, there has been a dramatic increase in interest in the functionality of protein radicals.[1] However, elucidating the reaction mechanisms of radical-containing proteins or understanding radiation damage to a protein requires a detailed knowledge of the chemistry and properties of amino acid radicals. Glycine, the simplest amino acid, is often used as an experimental model system[2−13] in studies of oxidation and reduction reactions of irradiated amino acids.

In 1964, after some years of controversy, Morton[12] tentatively proposed that the end oxidation and reduction products of glycine were $^{+}NH_3C^{\bullet}HCOO^{-}$ (R1) and $^{\bullet}CH_2COO^{-}$ (R2′), respectively. It was later shown[8b] that the species observed was $^{\bullet}CH_2COOH$ (R2) rather than the radical anion $^{\bullet}CH_2COO^{-}$. In 1997, Brustolon et al.[4] assigned three newly observed hyperfine coupling tensors to radical $NH_2C^{\bullet}H_2$. In 1998, Sanderud et al.[2] showed this to be incorrect and proposed that the radical was $NH_2C^{\bullet}HCOOH$ (R3). In addition, they assigned three more observed hyperfine couplings to another conformer of $NH_2C^{\bullet}$-HCOOH. The two experimentally observed conformers of $NH_2C^{\bullet}HCOOH$ are denoted hereafter as R3$^{\#}$ and R3*. In the paper of Sanderud et al.,[2] they correspond to Radical IV and Radical III, respectively. The H_α isotropic hyperfine coupling constants (HFCCs) of R3$^{\#}$ (−30.15 MHz) and R3* (−24.62 MHz) differ significantly. Based on the McConnell relation[14] and the Gordy-Bernhard[15] method, the smaller absolute isotropic HFCC in the proposed R3* was ascribed to nonplanarity of the radical center in the glycine crystal. Furthermore, experimental data[2] was used to suggest a twist angle of 24.2° between the OCO and CCN planes in R3*. This is an example for which experimental studies can only provide indirect information about the distortion of a radical in a specific environment. The assignment of complicated ESR spectra often requires simulations based on several assumptions. Hence, theoretical calculations of the HFCCs of amino acid radiation products can provide valuable assistance. The present study shows that correct identification of some radiation products of glycine-derived radicals can only be achieved through comparison of experimental and theoretical results. The glycine-derived radicals observed in irradiated glycine crystals at 280 K are shown in Figure 1.

In the gas-phase chemistry of amino acids, extensive G2-(MP2) calculations of thermochemical properties have been performed on glycine-derived radicals by Yu et al.[16] The ESR features of the glycine radical, $H_2NC^{\bullet}HCOOH$, have been studied previously at various levels of theory.[17,18] However, in the crystalline state and in solution, glycine exists as a zwitterionic species. The zwitterionic isomers of amino acids have been a challenge for theoretical chemistry. Ab initio calculations on glycine[19] and its radical[20,21] have shown that their zwitterionic structures do not correspond to energy minima in the gas phase. Environmental effects on the structure of R1 have previously been considered by performing a constrained geometry optimization[20] or by use of the conductor-like polarizable continuum model (CPCM).[21] Previously, calculations[21] on the isolated structure of R1 have shown that the isotropic HFCCs are not significantly influenced by the crystalline environment. In addition, it has been shown[22] that the Onsager model,[23,24] using the dielectric constant of water, yields the zwitterionic structure of the alanine radical $^{+}NH_3C^{\bullet}CH_3COO^{-}$ and that the resulting HFCCs are in good agreement with experiments.

Density functional theory has been shown to yield very accurate hyperfine coupling constants with great computational advantages.[25,26] Extensive DFT studies on the radicals formed in irradiated DNA bases and the sugar moiety have shown the success of DFT for biological systems.[27] In particular, promising DFT results on the alanine radical system[22,28] have prompted us to carry out a systematic study on glycine-derived radical species in order to obtain greater insight into the properties of irradiated amino acids.

Computational Methods

All geometry optimizations were performed with the B3LYP hybrid density functional in conjunction with the 6-31+G(d,p) basis set using the GAUSSIAN 98[29] suite of programs. The B3LYP functional is a combination of Becke's three-parameter hybrid exchange functional[30,31] and the Lee−Yang−Parr correlation functional.[32]

* To whom correspondence should be addressed. Email: boyd@is.dal.ca.

10.1021/jp993844h CCC: $19.00
Published on Web 04/29/2000

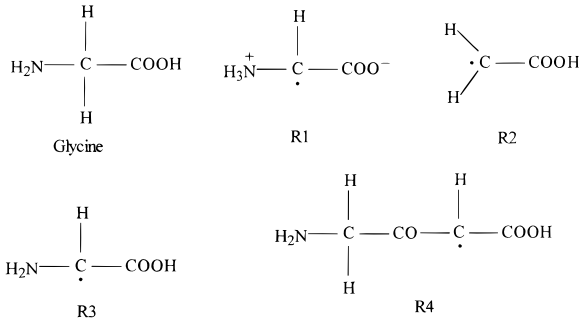

Figure 1. Schematic illustration of the structures of glycine and related radicals generated upon X-ray irradiation of glycine crystals at 280 K.

As noted previously, in solution and the crystalline state glycine is in its zwitterionic form, that is, $^{+}NH_3CH_2COO^{-}$. At the above level of theory, it is not computationally feasible to explicitly include the effects of the crytalline environment. However, one is able to obtain zwitterionic structures of glycine radicals using the standard Onsager model with a dielectric constant for water of 78.39. This approach, as noted in the Introduction, has been successfully used previously for alanine-derived radicals.[22]

All stationary points were confirmed to be local minima by harmonic vibrational frequency calculations at the same level of theory. Relative energies of all conformers of R2, R3, and R4 were obtained by performing single-point calculations at the B3LYP level in conjunction with the 6-311G(2df,p) basis set using the above optimized geometries and with inclusion of the appropriate zero-point vibrational energy correction (scaled by 0.9614[33]), that is, B3LYP/6-311G(2df,p)//B3LYP/6-31+G(d,p) + ZPVE.

Isotropic and anisotropic hyperfine coupling constant calculations were performed using the deMon program.[34] The PWP86 functional, a combination of Perdew and Wang's exchange functional (PW)[35] and Perdew's nonlocal correlation functional (P86),[36] in conjunction with the 6-311G(2d,p) basis set was employed. The (5,4;5,4) family of auxiliary basis sets was used to fit the charge density and the exchange correlation potential. This functional and basis set combination has been shown to give accurate hyperfine coupling constants in studies of alanine,[22] histidine,[37] and model π-radicals.[38]

Many assessments of methods for accurate calculation of hyperfine coupling constants have been previously published.[25,26,39] Hence, they shall not be reviewed here. However, it should be noted that accurate isotropic HFCCs require both a good description of electron correlation and a suitable basis set, whereas satisfactory anisotropic HFCCs are obtained at fairly low levels of theory, provided that the structure is qualitatively correct. Thus, comparison of anisotropic hyperfine tensors can be used as a reliable guide to identify radicals when less satisfactory agreement is obtained for the isotropic coupling constants.

B3LYP/6-31+G(d,p) optimized geometries in Cartesian coordinates and total energies of all species described in this study are presented in Table S1 of the Supporting Information.

Results and Discussion

The optimized geometries of R1, R2, R3, and R4 are shown schematically in Figure 2, whereas those of the experimentally proposed radicals R4′ ($^{+}NH_3CH_2COC^{\bullet}HCOO^{-}$) and R2′ ($^{\bullet}CH_2COO^{-}$) are shown schematically in Figure 3.

Geometry and Hyperfine Couplings of R1 ($^{+}NH_3C^{\bullet}HCOO^{-}$). The optimized zwitterionic structure of

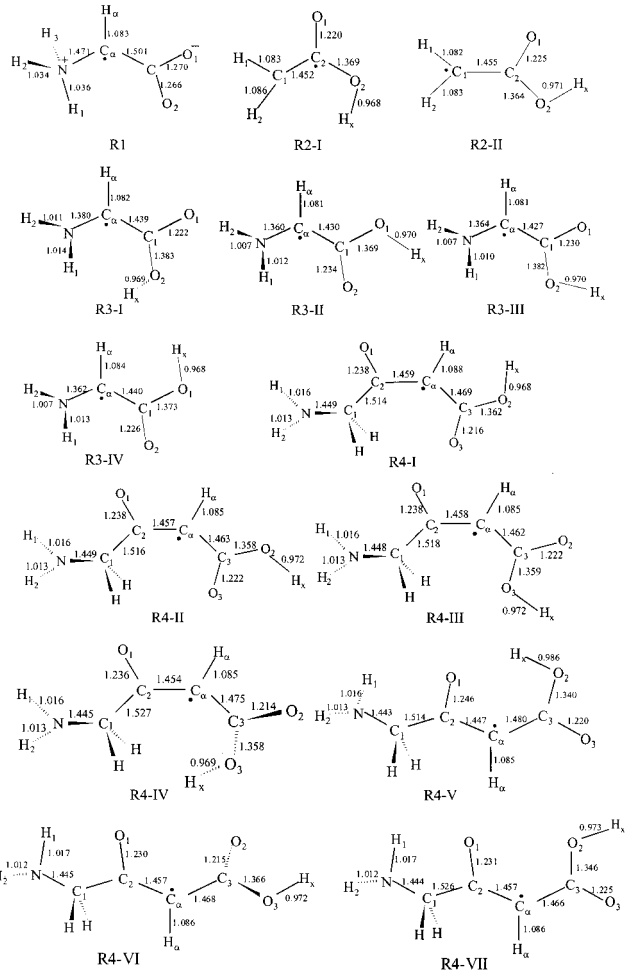

Figure 2. Optimized structures of R1, R2, R3, and R4 (bond lengths in angstroms).

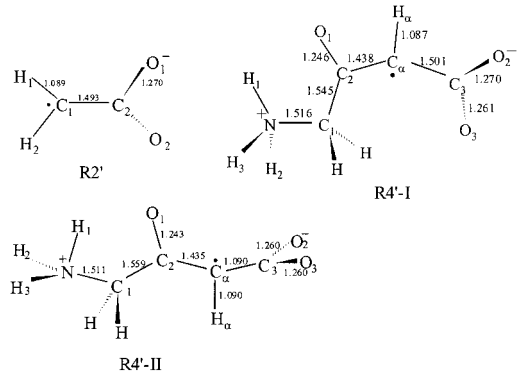

Figure 3. Optimized structures of R2′ and R4′ (bond lengths in angstroms).

R1 (Figure 2) was obtained using the Onsager model with an estimated radius of 3.24 Å. It possesses C_s symmetry with a planar radical center. Thus, R1 is a typical π-radical. The computed full hyperfine tensors of R1, as well as the experimental values and other previously calculated values, are listed in Table 1. The H_α isotropic HFCC is in good agreement with the experimental value. Similarly, the anisotropic components agree well with the experimental values, although the sign of T_{yy} differs from T_{yy}^{exp} due to its small value. In addition, comparison of the calculated (−95.0, −60.4, −21.5) and the experimental (−97.5, −61.9, −31.8) principal components shows that only the A_{zz} component is difficult to reproduce.

TABLE 1: PWP86/6-311G(2d,p) Calculated and Experimental HFCCs (MHz) of R1

tensor	A_{iso}	T_{xx}	T_{yy}	T_{zz}	A_{iso}^{exp}	T_{xx}^{exp}	T_{yy}^{exp}	T_{zz}^{exp}	A_{iso}[e]
H_α	−58.96	−36.06	−1.46	37.51	−63.72[a]	−33.80[a]	1.85[a]	31.94[a]	−60.3
H_1	2.33	−5.39	−4.66	10.05	3.3[b]	−7.3[b]	−1.8[b]	9.2[b]	
H_2	77.06	−5.47	−4.52	9.99	62.91[a]	−6.60[a]	−4.07[a]	10.66[a]	
H_3	77.06	−5.47	−4.52	9.99	83.05[a]	−5.86[a]	−4.80[a]	10.65[a]	
H_{ave}	52.15	−5.44	−4.57	10.01	49.07[a]	−2.93[a]	−2.05[a]	4.97[a]	52.1
C_α	98.73	−76.29	−74.57	150.87	126.7[c]	−90.0[c]	−36.7[c]	126.8[c]	95.3
N	−6.96	−0.43	0.20	0.22	−8.72[d]	−0.98[d]	−0.76[d]	1.71[d]	−9.0

[a] Ref 2. [b] Ref 11. [c] Ref 12. [d] Ref 10. [e] Ref 21 (B3LYP/EPR-2 calculated values).

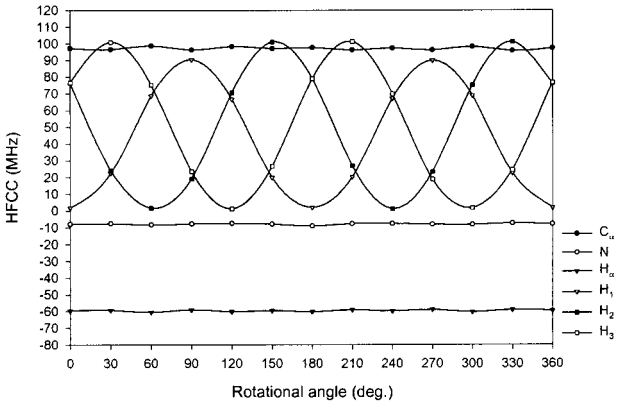

Figure 4. Variation of H_α, H_1, H_2, H_3, C_α, and N isotropic HFCCs of R1 with rotation of the amino group.

The anisotropic components of the hyperfine tensors of the three amino hydrogens (H_1, H_2, and H_3) are in good agreement with the experimental values. The isotropic HFCCs of H_1, H_2, and H_3 are of similar magnitude as experimental values, with the largest differences of 14.15 and 5.99 MHz being observed for H_2 and H_3, respectively. The isotropic HFCC and anisotropic components of the nitrogen are in good agreement with the experimental values. It can be seen that the calculated C_α HFCC at the PWP86/6−311(2d,p) level is in fair agreement with the experimental value and slightly better than a previous B3LYP/EPR-2 calculated value.[21] The B3LYP/EPR-2 study[21] has shown that the deviation of C_α HFCC based on the optimized zwitterionic structure can be significantly corrected by including the effect of vibrational averaging. The HFCCs of H_α and N, however, are not sensitive to vibrational averaging. Experimentally, the sign of the N hyperfine coupling has not been determined; however, it has been suggested to be negative.[8a,10,13b] This is supported by previous theoretical studies[20,21] and by the present results. In addition, an investigation[28] for the analogous alanine radical, $^+NH_3C^\bullet CH_3COO^-$, obtained a negative sign for the N HFCC.

The average (52.15 MHz) of the isotropic HFCCs of the three amino protons is in good agreement with the experimentally observed value of 49.07 MHz at 280 K, suggesting that the amino group rotates freely at 280 K. Furthermore, it also suggests that at 100 K, the orientation of the amino group in glycine crystals is constrained, giving rise to the three specific HFCC tensors of amino protons. Therefore, a detailed investigation was undertaken on the effects on the isotropic HFCCs of H_1, H_2, H_3, H_α, C_α, and N of rotating the amino group about the N—C_α bond of R1. The variation of the isotropic HFCCs as a function of the rotational angle is shown in Figure 4. The rotation of the amino group was carried out by incrementally increasing the dihedral angle $\angle H_1NC_\alpha C$ by 30°, starting from $\angle H_1NC_\alpha C = 0°$. From Figure 4, it can be seen that the isotropic HFCCs of H_1, H_2, and H_3 change dramatically, similar to that observed in the zwitterionic radical of alanine.[22] However, the isotropic couplings of H_α, C_α, and N are almost constant. It is noted that the difference in amplitude of the variation of the HFCC of H_1 and those of H_2 and H_3 is due to the fact that the geometrical parameters of the amino group have been constrained during rotation.

TABLE 2: PWP86/6-311G(2d,p) Calculated and Experimental[a] HFCCs (MHz) of R2-I, R2-II, and R2′ and Calculated[b] Relative Energies (kJ mol^{-1}) of R2-I and R2-II

					exptl	
tensor	HFCC	R2-I	R2-II	R2′	140 K	77 K
H_1	A_{iso}	−57.23	−57.71	−47.2	−58.9	−59.5
	T_{xx}	−33.30	−33.79	−32.9	−33.1	−34.0
	T_{yy}	−2.06	−2.07	−0.4	0.4	0.4
	T_{zz}	35.36	35.86	33.3	32.7	33.6
H_2	A_{iso}	−55.76	−57.24	−46.6	−55.8	−58.6
	T_{xx}	−34.66	−34.59	−33.0	−33.9	−33.9
	T_{yy}	−1.28	−1.68	−0.4	1.2	1.7
	T_{zz}	35.94	36.28	33.3	32.6	32.2
H_x	A_{iso}	−1.69	−4.09			0.48
	T_{xx}	−3.97	−2.78			−6.48
	T_{yy}	−2.08	−2.41			−3.75
	T_{zz}	6.04	5.19			10.27
ΔE		23.4	0.0			

[a] Ref 8b. [b] B3LYP/6-311G(2df,p)//B3LYP/6-31+G(d,p) + ZPVE.

When the amino group is rotated by approximately 5°, the isotropic HFCCs of H_2 and H_3 are in good agreement with the experimental values 62.91 and 83.05 MHz at 100 K, whereas the isotropic HFCC of H_1 is still less than 5 MHz. These results support the fact[2] that only the hyperfine splittings of two of the three constrained amino protons are easily observed, whereas the third remains too small to be distinguished from the many lines observed in the ENDOR spectra. Thus, from the HFCC calculations for the isolated R1, it can be concluded that the crystalline environment has little direct effect on the ESR spectra of R1, similar to the conclusion of a previous study.[21]

Geometry and Hyperfine Structure of R2 ($^\bullet CH_2COOH$). In 1964, Morton[12] concluded that the second radical observed in irradiated glycine crystals was the radical anion $^\bullet CH_2COO^-$ (R2′ in Figure 3) with only one H_α hyperfine coupling due to two equivalent hydrogens. However, Teslenko et al.[8b] reported that two forms of $^\bullet CH_2COOH$ (R2 in Figure 2) were observed: one at 77 K, the other at 140 K. Three inequivalent hyperfine couplings were observed for the conformer at 77 K, whereas two were observed for the conformer at 140 K. Recently, similar hyperfine structures were observed[2] at 100 K with the ambiguous conclusion that the radical may be either $^\bullet CH_2COO^-$ or $^\bullet CH_2COOH$. To clarify this ambiguity, calculations were performed on both species. The optimized structures of R2 and R2′ are shown in Figures 2 and 3, respectively. Two conformers of $^\bullet CH_2COOH$, R2-I and R2-II (Figure 2), were found. R2-I is almost planar, whereas R2-II is planar. Due to the existence of intramolecular hydrogen bonding, R2-II lies 23.4 kJ mol^{-1} lower in energy than R2-I (see Table 2). Interestingly, it was found that R2′ is not planar; both oxygen atoms lie out of the $H_1C_1H_2$ plane. However, R2′ was found to possess C_2 symmetry with a planar radical center.

TABLE 3: PWP86/6-311G(2d,p) Calculated HFCCs (MHz) of R3-I, R3-II, R3-III, R3-IV, the Experimental[a] Values of R3[#] and R3*, and Calculated[b] Relative Energies (kJ mol^{-1}) of R3-I, R3-II, R3-III and R3-IV

						exptl	
tensor	HFCC	R3-I	R3-II	R3-III	R3-IV	(R3[#])	(R3*)
H_α	A_{iso}	−40.41	−36.10	−38.03	−37.61	−30.15	−24.62
	T_{xx}	−24.95	−22.26	−22.36	−23.47	−17.24	−16.22
	T_{yy}	−2.04	−2.14	−2.06	−1.38	−0.19	−1.54
	T_{zz}	26.99	24.40	24.42	24.85	17.48	17.77
H_1	A_{iso}	25.04	−17.01	−16.39	−16.02	−18.05	−16.87
	T_{xx}	−12.60	−16.08	−15.81	−14.96	−16.00	−17.25
	T_{yy}	−5.52	−6.45	−5.04	−5.74	−4.18	−4.37
	T_{zz}	18.12	22.53	20.85	20.70	20.28	21.62
H_2	A_{iso}	−12.78	−14.27	−14.78	−10.70	−16.79	−15.46
	T_{xx}	−13.99	−19.26	−17.60	−18.02	−15.39	−16.42
	T_{yy}	−4.83	−5.42	−4.54	−4.65	−2.94	−3.99
	T_{zz}	18.82	24.67	22.15	22.67	18.34	20.40
ΔE		43.0	0.0	5.8	23.4		

[a] Ref 2. [b] B3LYP/6-311G(2df,p)//B3LYP/6-31+G(d,p) + ZPVE.

The calculated and experimental hydrogen HFCC tensors of R2′, R2-I, and R2-II are listed in Table 2. For R2-I and R2-II, the isotropic HFCCs and anisotropic components of H_1 and H_2 in R2-I are closest to the experimental values[8b] of the conformer observed at 140 K, whereas the isotropic HFCCs and anisotropic components of H_1 and H_2 in R2-II are in closest agreement with the experimental values[8b] of the conformer observed at 77 K (Table 2). The isotropic coupling and anisotropic components of H_x in both R2-I and R2-II are in reasonable agreement with the experimental values for the conformer observed at 77 K. In the case of R2′, the anisotropic components of H_1 and H_2 of R2′ are in good agreement with the experimental values of both observed conformations. However, the isotropic HFCCs of H_1 and H_2 of R2′ differ significantly from the experimental HFCCs of both conformers at 77 and 140 K. Thus, it can be concluded that neither of the conformations observed at 77 and 140 K is R2′ but instead are either R2-I or R2-II. However, as the calculated H_1 and H_2 hyperfine tensors of R2-I and R2-II are too close to be definitively assigned, more elaborate theoretical studies incorporating specific crystal and temperature effects, beyond the scope of the present study, will be required in order to make more definitive assignments.

Geometry and Hyperfine Couplings of R3 ($NH_2C^{\bullet}HCOOH$). The four optimized conformers of $NH_2C^{\bullet}$-HCOOH (denoted as R3-I, R3-II, R3-III, and R3-IV) are shown in Figure 2. The backbones of R3-II, R3-III, and R3-IV are almost planar, with all hydrogen atoms close to the $C_1C_\alpha N$ plane. Due to the significant repulsion between H_x and H_1, R3-I is more distorted, with the two oxygen atoms being out of the $C_1C_\alpha N$ plane by more than 7.7°, whereas H_1 is distorted out of the $C_1C_\alpha N$ plane by 36.3°. Accordingly, the radical centers in R3-II, R3-III, and R3-IV are less pyramidal than in R3-I. The relative energies in Table 3 show that R3-II and R3-III, with intramolecular hydrogen bonding, are more stable than R3-I and R3-IV.

The computed HFCC tensors in R3-I, R3-II, R3-III, and R3-IV and the experimental HFCC tensors of R3[#] and R3* are listed in Table 3. It is noted that the calculated isotropic HFCCs of the amino protons of R3-II differ significantly from previously calculated values.[18] This difference is most probably due to differences in the DFT optimized geometries used for the HFCC calculations. The optimized geometry obtained as part of this study is in closer agreement with higher-level ab initio calculations, suggesting that the presently calculated HFCCs should be more reliable.

From careful comparison of the calculated HFCCs for the four conformers of R3, they can be divided into two groups, with R3-I in one group and the rest in a second group. The isotropic HFCCs of H_α in R3-II, R3-III, and R3-IV are all in similar agreement with the experimental value of R3[#], differing by 6−8 MHz; however, they differ significantly from the experimental value of R3* by at least 12 MHz. The anisotropic components of the H_α HFCC tensor for the above conformers are in similar agreement with the experimental values of both R3[#] and R3*. Except for the isotropic HFCC of H_1 in R3-IV, the isotropic HFCCs and anisotropic components of the two amino protons of R3-II, R3-III, and R3-IV are in good agreement with the corresponding experimental values of both R3[#] and R3*, which are themselves very similar. Larger deviations were found between the calculated isotropic and anisotropic HFCCs of H_α and the experimental values of R3[#] or R3* in R3-I than in R3-II to R3-IV. It was found that the computed amino-proton isotropic H_1 HFCCs (25.03 MHz) in R3-I and the experimental values R3[#] and R3* (−18.05 and −16.87 MHz, respectively) are of the same magnitude; however, their signs are opposite. In addition, the anisotropic components of H_2 in R3-I are in less agreement with the experimental values than those of H_2 in the second group. Thus, R3-I could be neither R3[#] nor R3*. Although the above calculations using gas-phase optimized structures of R3 could not distinguish between R3[#] and R3*, we conclude that R3[#] can be one conformer or a mixture of R3-II, R3-III, and R3-IV. This is supported by the fact that R3-I is at least 20 kJ mol^{-1} higher in energy than the other three conformers of R3.

We note that the calculated H_α isotropic HFCCs of R3-II, R3-III, and R3-IV are in closer agreement with the experimental isotropic HFCC (33.0 MHz) of R3 in solution.[9] Hence, the deviation of the calculated H_α isotropic HFCCs of R3-II to R3-IV from the experimental values of R3[#] is likely due to crystal-packing effects, which are not taken into account by the above calculation.

An experimentally suggested[2] twist angle of 24.2° between the $NC_\alpha C_1$ and $O_1C_1O_2$ planes in R3* implies that the two amino protons and the two carboxylic oxygens are constrained by intermolecular hydrogen bonding. The effect of the two-plane twist on the H_α, H_1, and H_2 HFCCs of R3[#] was investigated by re-optimizing only H_α related geometrical parameters, that is, H_α—C_α, $\angle H_\alpha C_\alpha C_1$, and $\angle H_\alpha C_\alpha C_1 N$ in R3-II, R3-III, and R3-IV. The twisting of the $NC_\alpha C_1$ plane with respect to the $O_1C_1O_2$ plane was carried out by incrementally increasing the absolute value of $\angle O_2C_1C_\alpha N$ by 10° from 0°. The variation of the isotropic HFCCs of H_α, H_1, and H_2 with respect to the twist angle is shown in Figure 5.

It can be seen that the three plots exhibit the same pattern. The absolute isotropic HFCC of H_α decreases as the twist angle increases in R3-II, R3-III, and R3-IV. The isotropic HFCC of one amino proton (H_1) increases as the isotropic HFCC of the other amino proton (H_2) decreases in R3-II, R3-III, and R3-IV. As the isotropic HFCCs of H_1 and H_2 become equal (see Figure 5), the average ($H_{1,2}^{ave}$) of the isotropic HFCCs of H_1 and H_2 decreases slightly. However, the $H_{1,2}^{ave}$ values are all very close to the average of the experimental H_1 and H_2 isotropic couplings in R3* (16.16 MHz). It should be noted that by varying the twist angle, one is able to produce changes in the calculated H_α and $H_{1,2}^{ave}$ HFCCs, similar to the experimentally observed differences between R3[#] and R3* (see Table 3). Thus, although the calculations are unable to determine the conformation of R3*, they do support the experimental conclusion that R3* is

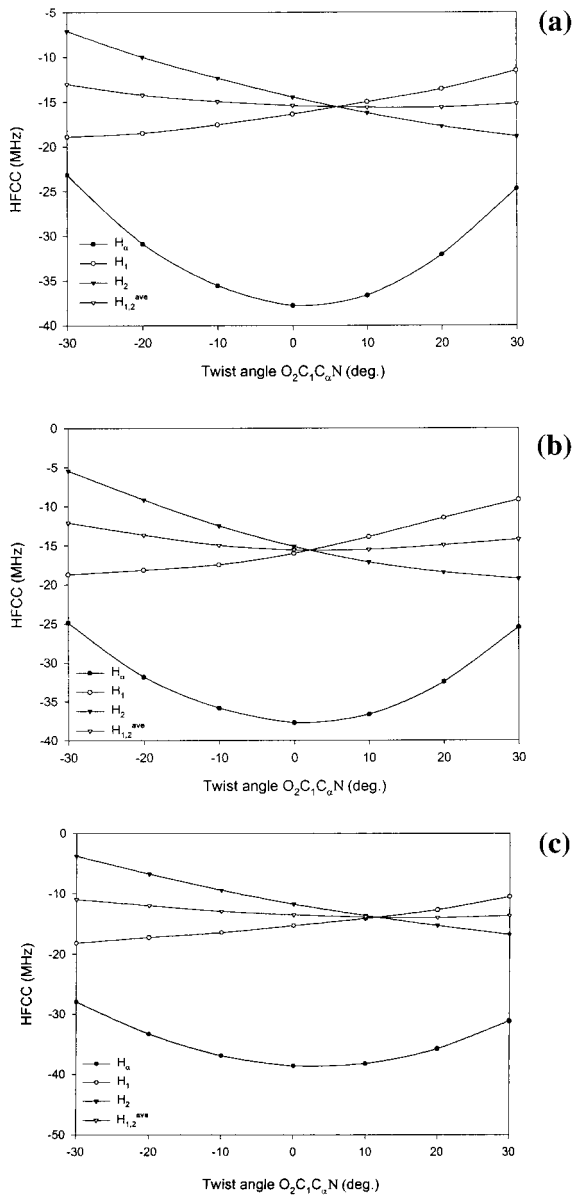

Figure 5. (a) Variation of H_α, H_1, H_2, and $H_{1,2}^{ave}$ isotropic HFCCs in R3-II with the twist angle $\angle O_2C_1C_\alpha N$. (b) Variation of H_α, H_1, H_2, and $H_{1,2}^{ave}$ isotropic HFCCs in R3-III with the twist angle $\angle O_2C_1C_\alpha N$. (c) Variation of H_α, H_1, H_2, and $H_{1,2}^{ave}$ isotropic HFCCs in R3-IV with the twist angle $\angle O_2C_1C_\alpha N$.

only a twisted configuration of R3# fixed by intermolecular hydrogen bonding in glycine crystals.

Protonation Effects on HFCCs in R3. To complete the theoretical studies of R3# and R3*, the corresponding protonated radical cation $NH_2C^{\bullet}HC(OH)_2^+$ ($R3^P$) was investigated. Optimized structures for conformers of $R3^P$ are shown in Figure 6. In $R3^P$-I and $R3^P$-III, the protonated carboxylic group is distorted slightly due to the repulsion between H_1 and H_{x2}; however, the radical centers are almost planar. $R3^P$-II is planar. In $R3^P$-IV, whereas the two oxygen atoms are distorted out of the $C_1C_\alpha N$ plane slightly by 2.7°, the rest, including the radical center C_α, remains planar. Comparison of the geometries of $R3^P$ with R3 suggests that protonation of R3 tends to make both the C_α and N centers more planar. However, the repulsion between H_1 and H_{x2} for a specific orientation can distort the planarity slightly. From the relative energies listed in Table 4, it can be seen that $R3^P$-II is the most stable conformer.

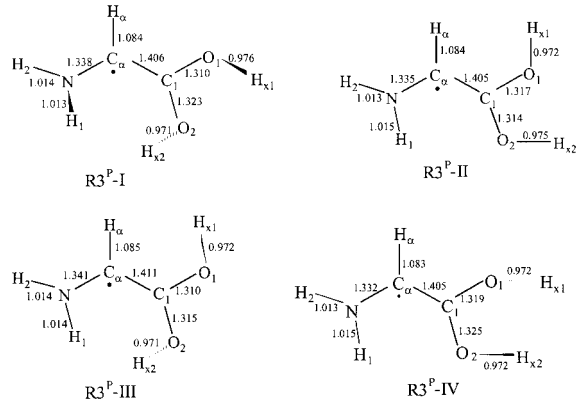

Figure 6. Optimized structures of $R3^P$ (bond lengths in angstroms).

TABLE 4: PWP86/6-311G(2d,p) Calculated HFCCs (MHz) of $R3^P$ Experimental[a] Values of R3*, and Calculated[b] Relative Energies (kJ mol^{-1}) of $R3^P$-I, $R3^P$-II, $R3^P$-III and $R3^P$-IV

tensor	HFCC	$R3^P$-I	$R3^P$-II	$R3^P$-III	$R3^P$-IV	exptl R3*
H_α	A_{iso}	−22.88	−22.89	−23.37	−21.74	−24.62
	T_{xx}	−13.55	−13.12	−14.70	−12.32	−16.22
	T_{yy}	−4.19	−3.73	−3.84	−4.04	−1.54
	T_{zz}	17.73	16.85	18.54	16.36	17.77
H_1	A_{iso}	−19.68	−24.09	−20.05	−22.87	−15.46
	T_{xx}	−17.38	−17.81	−17.50	−16.81	−16.42
	T_{yy}	−5.42	−5.91	−5.40	−5.73	−3.99
	T_{zz}	22.80	23.71	22.90	22.54	20.40
H_2	A_{iso}	−23.32	−25.04	−24.58	−24.17	−16.87
	T_{xx}	−19.27	−20.93	−19.36	−20.00	−17.25
	T_{yy}	−4.850	−5.02	−4.83	−4.74	−4.37
	T_{zz}	24.12	25.95	24.19	24.74	21.62
ΔE		22.1	0.0	38.2	10.1	

[a] Ref 2. [b] B3LYP/6-311G(2df,p)//B3LYP/6-31+G(d,p) + ZPVE.

The computed hyperfine coupling tensors in $R3^P$-I, $R3^P$-II, $R3^P$-III, and $R3^P$-IV are shown in Table 4. The isotropic HFCC and anisotropic components of H_α in each conformer are in agreement with the corresponding experimental values of R3*. However, the isotropic HFCCs of the two amino protons in $R3^P$-I, $R3^P$-II, $R3^P$-III, and $R3^P$-IV are slightly larger than the experimental isotropic HFCCs. Interestingly, the anisotropic components of the two amino protons in each conformer are in good agreement with the experimental values of R3*. The calculations suggest that to exclude the possibility that $R3^P$ is R3*, experimental studies of the carboxylic proton are required.

Enhanced Captodative Effects from Protonation on R3. It was postulated[40] that the complementary electron-withdrawing (capto) and electron-donating (dative) effect in R3 will enhance its stablization by delocalization of spin density and charge. It can be seen that $R3^P$ also has an electron-donating group $-NH_2$ and an electron-withdrawing group $-C(OH)_2^+$. To identify how the spin density delocalizes in captodative-type radicals, the spin density on the C, N, and O atoms of R3 and $R3^P$ were compared (see Table 5). It can be seen that more than 50% of the total spin is localized on C_α in R3, whereas the rest is mainly localized on the N and carbonyl O. It can be concluded that this type of spin distribution is due mainly to the effect of the spin polarization of the unpaired electron at C_α on the lone-pair electrons of the N and π electrons of the CO double bond of the carboxylic group. In $R3^P$, more than 80% of the spin density is almost equally shared between the N, C_α, and C_1 atoms, whereas the rest is shared by the two O atoms. Thus, the spin distribution in $R3^P$ is significantly different from that seen in R3. The spin density $\rho(C_\alpha) > \rho(C_1) > \rho(O_i)$, $(i = 1, 2)$, in $R3^P$ can be explained by the spin induction along the chemical

TABLE 5: PWP86/6-311G(2d,p) Calculated Spin Density on C, N, and O Atoms of R3 and R3^P

system	C_α	N	C_1	O_1	O_2	$O_1 + O_2$
R3-I	0.614	0.210	0.018	0.187	0.013	0.200
R3-II	0.507	0.291	0.079	0.033	0.146	0.179
R3-III	0.540	0.267	0.05	0.18	0.021	0.201
R3-IV	0.556	0.277	0.048	0.036	0.141	0.177
R3^P-I	0.313	0.315	0.239	0.115	0.067	0.182
R3^P-II	0.291	0.345	0.243	0.094	0.081	0.175
R3^P-III	0.351	0.322	0.213	0.107	0.063	0.170
R3^P-IV	0.268	0.329	0.272	0.103	0.077	0.180

TABLE 6: PWP86/6-311G(2d,p) Calculated HFCCs of R4′ and R4 with Experimental[a] Values and Calculated[b] Relative Energies (kJ mol^{-1})

system	A_{iso}	T_{xx}	T_{yy}	T_{zz}	ΔE
R4′-I	−12.15	−12.89	−4.38	17.27	
R4′-II	−20.34	−12.79	−1.99	14.77	
R4-I	−41.39	−24.82	−2.25	27.08	29.6
R4-II	−42.03	−24.65	−2.47	27.13	7.0
R4-III	−42.31	−23.76	−2.84	26.60	13.4
R4-IV	−41.37	−23.91	−3.26	27.17	42.1
R4-V	−41.72	−24.70	−2.47	27.17	0.0
R4-VI	−42.92	−26.46	−1.86	28.32	21.3
R4-VII	−42.27	−25.28	−2.32	27.60	18.8
exptl	−47.99	−25.03	1.29	23.73	

[a] Ref 2. [b] B3LYP/6-311G(2df,p)//B3LYP/6-31+G(d,p) + ZPVE.

bonds by the positive charge of $-C(OH)_2^+$. Furthermore, the strong electron-withdrawing capability of $-C(OH)_2^+$ in R3^P significantly enhances the spin polarization of the lone-pair electrons of the N atom. Hence, approximately 30% of the spin density resides on the N. Thus, spin induction and spin polarization together explain the spin distribution $\rho(C_\alpha) \sim \rho(N) > \rho(C_\alpha) > \rho(C_1) > \rho(O_1) \sim \rho(O_2)$ in R3^P.

Geometry and Hyperfine Coupling of R4 ($NH_2CH_2COC^{\bullet}HCOOH$). The detection of R4 is a new finding[2] in the radiation chemistry of glycine crystals at room temperature. Experiments[2] confidently showed that there is only one H_α coupling tensor in R4 without any other α- and β-proton couplings. This fact prompted Sanderud et al.[2] to propose a zwitterionic structure (R4′) for the dimeric-type radical and to propose a mechanism for the formation of R4′ from the reaction of zwitterionic glycine with R2′. We consider that an assignment of the observed couplings to the correct radiation products is essential for further mechanistic studies. The optimized structures of two possible conformers of R4′, obtained using the Onsager model with an estimated radius of 4.16 Å, are shown schematically in Figure 3.

The carbons and nitrogen in R4′-I form an almost planar skeleton with an almost planar radical center. However, O_2 and O_3 lie out of the mean molecular plane by approximately 25°. In R4′-II, the carbons, N, and O_1 are coplanar. However, the $O_2C_3O_3$ plane is almost perpendicular to the plane of the molecular skeleton.

The calculated hyperfine coupling tensors of H_α in R4′-I and R4′-II, as well as the experimental values, are listed in Table 6. It can be seen that both the isotropic HFCC and anisotropic components of H_α in R4′-I and R4′-II differ significantly from the corresponding experimental values. Thus, it is unlikely that R4′ is the radical experimentally observed. However, it is quite possible that R4′ is in fact not in its zwitterionic form. Hence, the neutral radical $NH_2CH_2COC^{\bullet}HCOOH$ (R4) was also investigated. Seven conformers of R4 were located; their optimized structures are shown schematically in Figure 2.

There are significant skeletal differences between the structures of R4-I to R4-IV and those of R4-V to R4-VII. The four carbon atoms in R4-I to R4-IV form cis structures, whereas the four carbon atoms in R4-V to R4-VII form trans structures. The main difference among R4-I, R4-II, R4-III, and R4-IV, as well as among R4-V, R4-VI, and R4-VII, is the bonding position and orientation of H_x. The radical center in R4-I, R4-II, R4-III, R4-V, R4-VI, and R4-VII is almost planar, whereas the radical center in R4-IV ($\angle H_\alpha C_\alpha C_3 C_2 = -172.6°$) is distorted by approximately 8° due to repulsion between H_x and the hydrogen on C_1. In addition, O_2 and O_3 in R4-IV lie out of the $C_3C_\alpha H_\alpha$ plane by 29.4°.

The calculated HFCC tensors of H_α in R4-I to R4-VII are listed in Table 6. It can be seen that both the isotropic HFCC and anisotropic components of the H_α tensor in R4-I to R4-VII are in close agreement with the corresponding experimental values. Thus, it can be concluded that the experimentally observed radical must be R4 and not R4′. Correspondingly, R4 should be formed from the reaction of the zwitterionic form of glycine with R2 rather than with R2′. Thus, a deprotonation of the amino group in the zwitterionic form of glycine must be involved. However, to determine the conformation of R4 and the mechanism by which it is formed, more experimental and theoretical investigations of the radical are required.

Conclusions

The geometries and hyperfine couplings of the four observed radicals generated from irradiated glycine crystals were computed using density functional theory. The calculated HFCCs were compared with experimental values obtained at 295, 100, and 77 K.

A zwitterionic structure of R1 with C_s symmetry was predicted using the Onsager model. The H_α couplings and the average HFCC of the three amino protons are in good agreement with the experimental values, supporting the observation that the amino group in glycine rotates freely at room temperature. A detailed study of the effect of rotating the amino group on the proton HFCCs showed that at 100 K, the amino group of R1 is constrained by intermolecular hydrogen bonding to be approximately 5° away from the optimized structure. The small value of the H_1 isotropic HFCC when the rotational angle is 5° supports the fact that the HFCC of one of the three amino protons is too small to be distinguished by the ENDOR technique at 100 K. In addition, the rotation of the amino group was found to have little effect on the HFCCs of H_α, C_α, and N in R1.

Two conformers of $^{\bullet}CH_2COOH$ (R2-I and R2-II) were found, which are able to account for the two forms of R2 observed experimentally, one at 77 K and the other at 140 K. The hyperfine coupling constants of the alternatively suggested radical R2′ ($^{\bullet}CH_2COO^-$) differ significantly from those observed experimentally. However, the present calculations are unable to unambiguously assign R2-I or R2-II to either experimentally observed conformer.

The HFCCs of three of the four possible conformations of R3 account for the experimental values of R3$^{\#}$. However, the deviation of the calculated isotropic HFCC of H_α from experiments suggests that the crystal packing in glycine has a significant effect on the H_α hyperfine coupling constant of R3$^{\#}$. HFCC calculations on the re-optimized structures of R3, with appropriate geometrical constraints, support the experimental postulate that the major difference between the two conformations of R3 is the twist between the $O_1C_1O_2$ and $C_1C_\alpha N$ planes.

HFCC calculations on the experimentally proposed zwitterionic structure of R4′ obtained with the Onsager model differ significantly from the experimental values, showing that R4′

could not be the radical observed. However, the seven conformers of R4 all give HFCCs in good agreement with the experimental values. Hence, it is more likely that the radical observed experimentally is R4 (ie., nonzwitterionic form). Thus, when it is formed from the reaction of the zwitterionic form of glycine with R2, a deprotonation of the amino group in the zwitterionic form of glycine must be involved.

With respect to the theoretical methods employed, it can be seen again that density functional theory is successful in predicting the magnetic properties of amino acids. Furthermore, the Onsager model is found to work as equally well for the glycine radical in its zwitterionic form as previously found for the alanine radical system, resulting in structures capable of reproducing the experimental hyperfine coupling constants.

Acknowledgment. We gratefully acknowledge the Natural Sciences and Engineering Research Council of Canada (NSERC) and the Killam Trusts for financial support and thank Drs. Stacey D. Wetmore and Leif A. Eriksson for helpful discussions.

Supporting Information Available: B3LYP/6-31+G(d,p) optimized geometries in Cartesian coordinates and total energies for all radicals in the present study (Table S1) are available (12 pages). This material is available free of charge via the Internet at http://pubs.acs.org.

References and Notes

(1) (a) Stubbe, J.; Donk, W. A. v. *Chem. Rev.* **1998**, *98*, 705. (b) Stubbe, J. *Annu. Rev. Biochem.* **1989**, *58*, 257. (c) Stubbe, J. *Biochemistry* **1988**, *27*, 3893.

(2) Sanderud, A.; Sagstuen, E. *J. Phys. Chem. B* **1998**, *102*, 9353.

(3) Bonifacic, M.; Stefanic, I.; Hug, G. L.; Armstrong, D. A.; Asmus, K. *J. Am. Chem. Soc.* **1998**, *120*, 9930.

(4) Brustolon, M.; Chis, V.; Maniero, A. L.; Brunel, L.-C. *J. Phys. Chem. A* **1997**, *101*, 9763.

(5) Syutkin, V. M.; Tolkachev, V. A. *Radiat. Phys. Chem.* **1982**, *20*, 281.

(6) Box, H. C. *Radiation Effects: ESR and ENDOR Analysis*; Academic Press: New York, 1977.

(7) (a) Muto, H.; Iwasaki, M.; Takahashi, Y. *J. Chem. Phys.* **1977**, *66*, 1943. (b) Nunome, K.; Muto, H.; Toriyama, K.; Iwassaki, M. *J. Chem. Phys.* **1976**, *65*, 3805. (c) Iwassaki, M.; Muto, H. *J. Chem. Phys.* **1974**, *61*, 5315.

(8) (a) Deigen, M. F.; Krivenko, V. G.; Pulatova, M. K.; Ruban, M. A.; Teslenko, V. V.; Kayushin, L. P. *Biofisika* **1973**, *18*, 235. (b) Teslenko, V. V.; Gromovoi, Y. S.; Krivenko, V. G. *Mol. Phys.* **1975**, *30*, 425.

(9) Neta, P.; Fessenden, R. W. *J. Phys. Chem.* **1971**, *75*, 738.

(10) Hedberg, A.; Ehrenberg, A. *J. Chem. Phys.* **1968**, *48*, 4822.

(11) Collins, M. A.; Whiffen, D. H. *Mol. Phys.* **1966**, *10*, 317.

(12) Morton, J. R. *J. Am. Chem. Soc.* **1964**, *86*, 2325.

(13) (a) Ghosh, D. K.; Whiffen, D. H. *J. Chem. Soc.* **1960**, 1869. (b) Ghosh, D. K.; Whiffen, D. H. *Mol. Phys.* **1959**, *2*, 285.

(14) McConnell, H. M. *J. Chem. Phys.* **1956**, *24*, 764.

(15) (a) Gordy, W. *Theory and Applications of Electron Spin Resonance*; John Wiley & Sons: New York, 1980. (b) Bernhard, W. A. *J. Chem. Phys.* **1965**, *24*, 764.

(16) Yu, D.; Rauk, A.; Armstrong, D. A. *J. Am. Chem. Soc.* **1995**, *117*, 1789.

(17) Barone, V.; Adamo, C.; Grand, A.; Jolibois, F.; Brunel, Y.; Subra, R. *J. Am. Chem. Soc.* **1995**, *117*, 12618.

(18) Himo, F.; Eriksson, L. A. *J. Chem. Soc., Perkin Trans. 2* **1998**, 305.

(19) Ding, Y.; Krogh-Jespersen, K. *Chem. Phys. Lett.* **1992**, *199*, 261.

(20) Barone, V.; Adamo, C.; Grand, A.; Subra, R. *Chem. Phys. Lett.* **1995**, *242*, 351.

(21) Rega, N.; Cossi, M.; Barone, V. *J. Am. Chem. Soc.* **1998**, *120*, 5723.

(22) Ban, F.; Wetmore, S. D.; Boyd, R. J. *J. Phys. Chem.* A **1999**, *103*, 4303.

(23) Onsager, L. *J. Am. Chem. Soc.* **1936**, *58*, 1486.

(24) (a) Wong, M. W.; Frisch, M. J.; Wiberg, K. B. *J. Am. Chem. Soc.* **1991**, *113*, 4776. (b) Wong, M. W.; Wiberg, K. B.; Frisch, M. J. *J. Am. Chem. Soc.* **1992**, *114*, 523. (c) Wong, M. W.; Wiberg, K. B.; Frisch, M. J. *J. Am. Chem. Soc.* **1992**, *114*, 1645. (d) Wong, M. W.; Wiberg, K. B.; Frisch, M. J. *J. Chem. Phys.* **1991**, *95*, 8991.

(25) Malkin, V. G.; Malkina, O. L.; Eriksson, L. A.; Salahub, D. R. In *Modern Density Functional Theory, A Tool for Chemistry*; Politzer P., Seminario, J. M., Eds.; Elsevier: New York, 1995; p 273.

(26) Engels, B.; Eriksson, L. A.; Lunell, S. *Adv. Quantum Chem.* **1997**, *27*, 298.

(27) (a) Wetmore, S. D.; Boyd, R. J.; Eriksson, L. A. *J. Phys. Chem.* B **1998**, *102*, 5369. (b) Wetmore, S. D.; Himo, F.; Boyd, R. J.; Eriksson, L. A. *J. Phys. Chem.* B **1998**, *102*, 7484. (c) Wetmore, S. D.; Boyd, R. J.; Eriksson, L. A. *J. Phys. Chem.* B **1998**, *102*, 7674. (d) Wetmore, S. D.; Boyd, R. J.; Eriksson, L. A. *J. Phys. Chem. B* **1998**, *102*, 9332. (e) Wetmore, S. D.; Boyd, R. J.; Eriksson, L. A. *J. Phys. Chem. B* **1998**, *102*, 10602.

(28) Lahorte, P.; Proft, F. D.; Vanhaelewyn, G.; Masschaele, B.; Cauwels, P.; Callens, F.; Geerlings, P.; Mondelaers, W. *J. Phys. Chem. A* **1999**, *103*, 6650.

(29) Frisch, M. J.; Trucks, G. W.; Schlegel, H. B.; Scuseria, G. E.; Robb, M. A.; Cheeseman, J. R.; Zakrzewski, V. G.; Montgomery, J. A.; Stratmann, R. E.; Burant, J. C.; Dapprich, S.; Millam, J. M.; Daniels, A. D.; Kudin, K. N.; Strain, M. C.; Farkas, O.; Tomasi, J.; Barone, V.; Cossi, M.; Cammi, R.; Mennucci, B.; Pomelli, C.; Adamo, C.; Clifford, S.; Ochterski, J.; Petersson, G. A.; Ayala, P. Y.; Cui, Q.; Morokuma, K.; Malick, D. K.; Rabuck, A. D.; Raghavachari, K.; Foresman, J. B.; Cioslowski, J.; Ortiz, J. V.; Stefanov, B. B.; Liu, G.; Liashenko, A.; Piskorz, P.; Komaromi, I.; Gomperts, R.; Martin, R. L.; Fox, D. J.; Keith, T. A.; Al-Laham, M. A.; Peng, C. Y.; Nanayakkara, A.; Gonzalez, C.; Challacombe, M.; Gill, P. M. W.; Johnson, B. G.; Chen, W.; Wong, M. W.; Andres, J. L.; Head-Gordon, M.; Replogle, E. S.; Pople, J. A. GAUSSIAN 98; Gaussian, Inc.: Pittsburgh, PA, 1998.

(30) Becke, A. D. *J. Chem. Phys.* **1993**, *98*, 1372.

(31) Stephens, P. J.; Devlin, F. J.; Frisch, M. J.; Chabalowski, C. F. *J. Phys. Chem.* **1994**, *98*, 11623.

(32) Lee, C.; Yang, W.; Parr, R. G. *Phys. Rev. B* **1988**, *37*, 785.

(33) Scott, A. P.; Radom, L. *J. Phys. Chem.* **1996**, *100*, 16502.

(34) (a) St-Amant, A.; Salahub, D. R. *Chem. Phys. Lett.* **1990**, *169*, 387. (b) Salahub, D. R.; Fournier, R.; Mylynarski, P.; Papai, I.; St-Amant, A.; Ushio, J. In *Density Functional Methods in Chemistry*; Labanowski, J., Andzelm, J., Eds.; Springer-Verlag: New York, 1993. (c) St-Amant, A. Ph.D. Thesis, Université de Montréal, 1991.

(35) Perdew, J. P.; Wang, Y. *Phys. Rev. B* **1986**, *33*, 8800.

(36) (a) Perdew, J. P. *Phys. Rev. B* **1986**, *33*, 8822. (b) Perdew, J. P. *Phys. Rev. B* **1986**, *34*, 7406.

(37) Lassmann, G.; Eriksson, L. A.; Himo, F.; Lendzian, F.; Lubitz, W. *J. Phys. Chem. A* **1999**, *103*, 1283.

(38) Eriksson, L. A. *Mol. Phys.* **1997**, *91*, 827.

(39) Gauld, J. W.; Eriksson, L. A.; Radom, L. *J. Phys. Chem. A* **1997**, *101*, 1352.

(40) Easton, C. J. *Chem. Rev.* **1997**, *97*, 53.